

Contents lists available at **CEPM**

Computational Engineering and Physical Modeling

Journal homepage: www.jcepm.com

Steel Plate Shear Wall with Different Infill Steel Plates

M.H. Kashefzadeh¹, M. Azimzadeh Koocheh², B. Amiri^{3*}, R. EsmailAbadi⁴

1. Ph.D. Candidate, Department of Civil Engineering, University of Arkansas, USA

2. Department of Civil Engineering, Kish International Branch, Islamic Azad University, Kish Island, Iran

3. Young Researchers Club, Roudehen Branch, Islamic Azad University, Roudehen, Iran

4. Assistant Professor, Department of Civil Engineering, Roudehen Branch, Islamic Azad University, Roudehen, Iran

Corresponding author: amiri.behtash@gmail.com



<https://doi.org/10.22115/CEPM.2018.118244.1011>

ARTICLE INFO

Article history:

Received: 06 February 2018

Revised: 15 May 2018

Accepted: 22 May 2018

Keywords:

Steel plate shear wall;

Finite element method;

Nonlinear behavior;

Pushover analysis.

ABSTRACT

The steel plate shear wall (SPSW) system is one of the most common and acceptable lateral-resisting structural systems for steel structures. Although the advantages of SPSW over the other structural systems are somehow well-known, the wall-frame interaction of the system is not comprehensively investigated. Therefore, the present study aims at investigating the interaction of the infill steel walls and the moment frames with RBS beams, using finite element method. For this purpose, different finite element model of SPSWs with various span lengths and infill steel plates are developed. The models have the low-yield, medium-yield, and high-strength infill steel plates. At first, eigenvalue buckling analysis is accomplished and those buckling mode shapes were used to introduce the initial imperfection for a realistic simulation. In the study, the important seismic parameters—including the lateral stiffness, the ultimate shear capacity, energy absorption, and ductility—are investigated using nonlinear pushover analysis. Finite element results of the study indicate utilizing the low-yield steel plate affects inversely the contribution to the wall-frame interaction and reduces significantly the shear capacity of SPSWs. However, using high-strength structural steel plate enhances the shear capacity. Moreover, using infill steel plates with different properties does not change the initial elastic stiffness of the shear wall. Additionally, increasing the span length of steel plate shear wall, the ultimate shear strength and energy dissipation increase significantly, but the ductility of the system decreases.

How to cite this article: Kashefzadeh MH, Azimzadeh Koocheh M, Amiri B, Esmailabadi R. Steel Plate Shear Wall with Different Infill Steel Plates. *Comput Eng Phys Model* 2018;1(3):1–14. <https://doi.org/10.22115/cepm.2018.118244.1011>

2588-6959/ © 2018 The Authors. Published by Pouyan Press.

This is an open access article under the CC BY license (<http://creativecommons.org/licenses/by/4.0/>).



1. Introduction

In the recent decades, steel plate shear walls (SPSW) have been widely used in steel structures to resist the lateral loads, both the earthquake and wind. SPSW are made of the infill steel plates surrounded by the beams and columns. The beams and columns in this system are called the boundary elements. SPSW acts like a cantilever plate girder, where its columns work as the flanges and the beams act as the stiffeners. In addition, the steel plates are the web of the plate girder. There are so many experimental, numerical, and analytical studies on SPSW which confirm the wall has a good seismic performance [1–10]. The construction of SPSW is similar to the steel structures and it is also possible to pre-fabricate the wall. Therefore, the implementation of SPSW is fast and easy in the real structures.

SPSW has higher seismic capacity than the other lateral load resisting systems in steel buildings. The primary reason of this excellent performance is that SPSW give higher shear capacity and ductility in resisting the lateral forces [1–5]. In addition, SPSW provide higher lateral stiffness that results in less drift compared with other systems. Steel structures with SPSW have lower structural weight, thus exerts less loads to the perimeter columns and the foundation. In fact, the lighter structure weight triggers the lower the seismic force. Furthermore, the homogenous of the materials of the shear wall improves the performance of the connections and leads to an enhanced structural behavior [5].

There are three major types of SPSW. The system can be used as stiffened, unstiffened, or in composition with reinforced concrete panels, which is called composite steel plate shear walls (CSPSW) [1,2,11–20,3,21–25,4–10]. In SPSW without stiffener, the infill steel plate buckling in compression field occurs due to small lateral force because the infill plate is thin. Therefore, the lateral forces are resisted by developing tension field action. This behaviour is similar to the plate girders with slender web plate. In SPSW with stiffener, the stiffeners increase the buckling capacity of the infill steel plate. Thus, the shear yield takes place in the infill plate. In CSPSW, the reinforced concrete panel also prevents the infill plate buckling, which can be used on one or both sides of the plate. Stiffened SPSW and CSPSW provide higher stiffness and shear strength [11–20].

In this study, the nonlinear response of wall-frame interaction of SPSW is numerically investigated. In the research, three different steel plates (low-yield, medium-yield, high-strength) are considered in design of shear walls. Four practical spans of 3m, 4.5m, 6m, and 7.5m are chosen. The seismic characteristics—shear capacity, lateral stiffness, and ductility of shear wall—are evaluated.

2. Analysis procedure

2.1. Finite element method

This section represents the finite element method of SPSW models used in this study. Commercial finite element software program, Abaqus, was used [26]. 4-node shell elements and 8-node solid elements were selected for the steel plate and boundary elements, respectively.

Solid elements were selected for boundary elements to capture the local inelastic buckling at the members. The shear wall models have 4 spans of 3, 4.5, 6, and 7.5m, and the infill steel plate height is 3m, as shown in Fig. 1. In design of the beams and columns of SPSW, the Seismic provision AISC341 and AISC Design Guide 20 were used. SPSW models have an internal steel plate of 3.42mm (0.1345 in). Fig. 1.b shows the details of a typical finite element model of SPSW. Moreover, Table 1 provides the details of the beams and columns of the model.

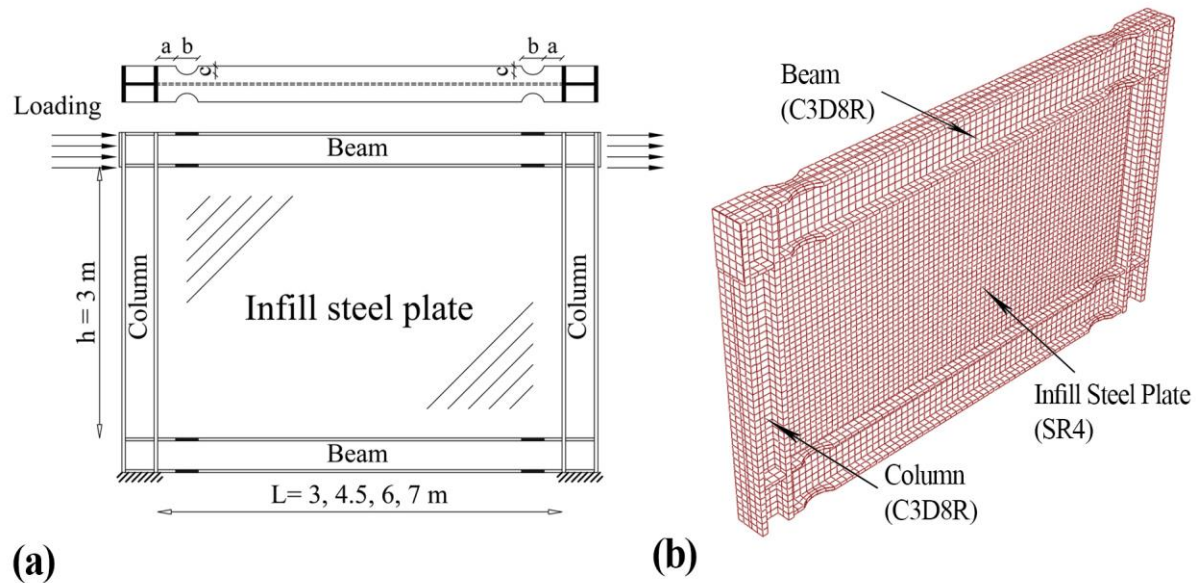


Fig. 1. A typical finite element of SPSW model.

Table 1
Specifications of the beams and columns in SPSW models.

Specimen	L (Cm)	H (Cm)	L/h	Infill steel plate (mm)	Beams	Columns	A (mm)	b (mm)	c (mm)
S3A1	300	300	1	3.42	W14x159	W14x211	200	250	95
S3A1.5	450	300	1.5	3.42	W14x311	W14x342	210	290	100
S3A2	600	300	2	3.42	W27x281	W14x426	185	485	90
S3A2.5	750	300	2.5	3.42	W36x395	W14x550	215	635	105

2.2. Material properties

In the numerical analysis, three different steel materials (low-yield, medium-yield, and high-strength) are considered for the steel plate. High-strength steel (A572) was used for beams and columns. Fig. 2 shows the material properties of structural steel. Low-yield steel (S100) has the yield stress of 100 Mpa and the Medium-yield (A36) steel has the yield stress of 245 MPa. High-strength steel (A572) with yield stress of 345 MPa is also used too. The modulus of elasticity and Poisson's ratio are 200 GPa and 0.3 respectively.

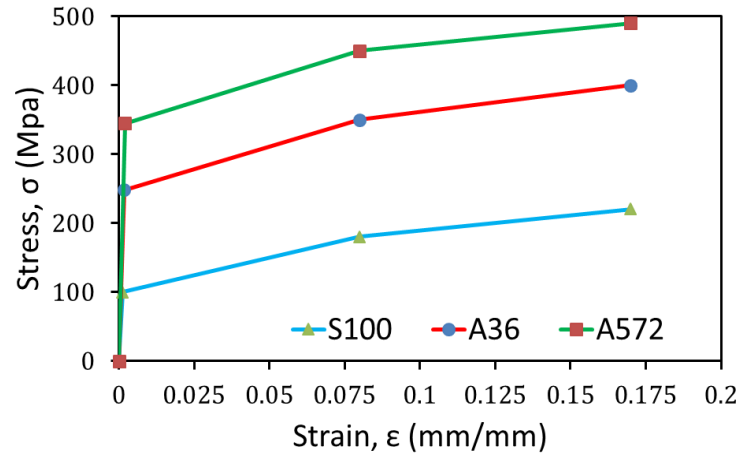


Fig. 2. Material properties of steel.

2.3. Buckling analysis

Before doing the nonlinear pushover analysis, the finite element models of SPSW were subjected to eigenvalue buckling analysis. The buckling analysis results of the infill steel plate were effectively used to introduce the initial imperfection for a more realistic simulation. The magnitude of the initial imperfection was $h/1000$, where h was the height of plate. In the nonlinear pushover analysis, the first mode of buckling was only used to impose the initial imperfection. Fig. 3 represent the 1st to 4th buckling modes of the infill plate of the web.

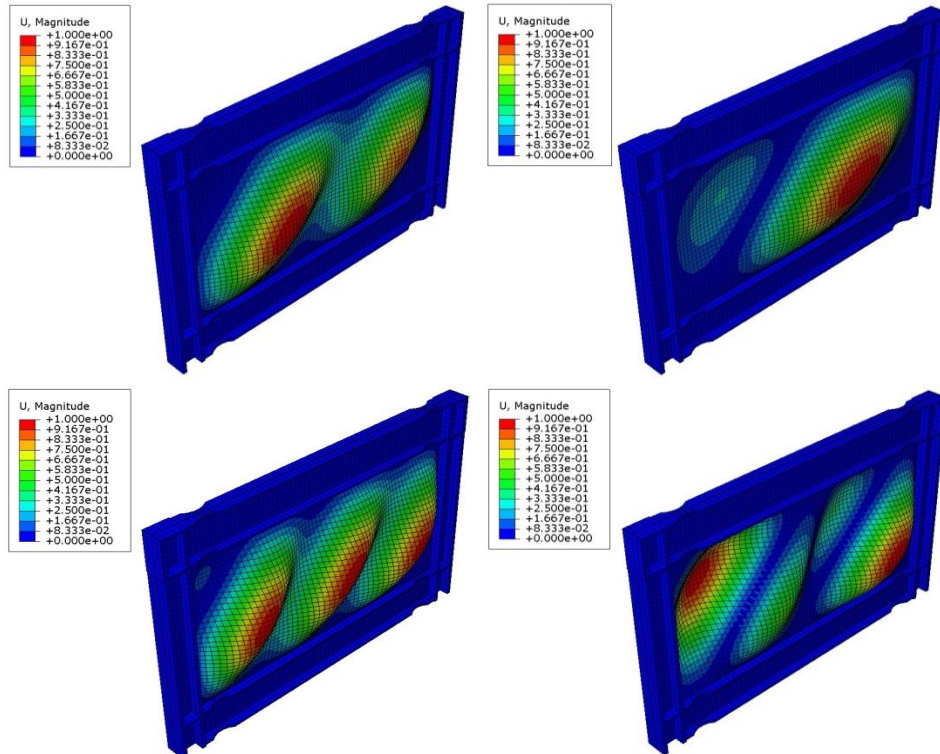


Fig. 3. Buckling analysis of steel plate shear wall.

2.4. Verification of finite element method

Finite element method was verified by comparing the results with experimental results. SPSW tested by Lubell et al. is selected for this study [24]. Fig. 4 shows the comparison that validate the finite element modelling. There is a good agreement in numerical modelling and experiment. Additionally, the buckling modes and failure of specimen was similar to the reported test.

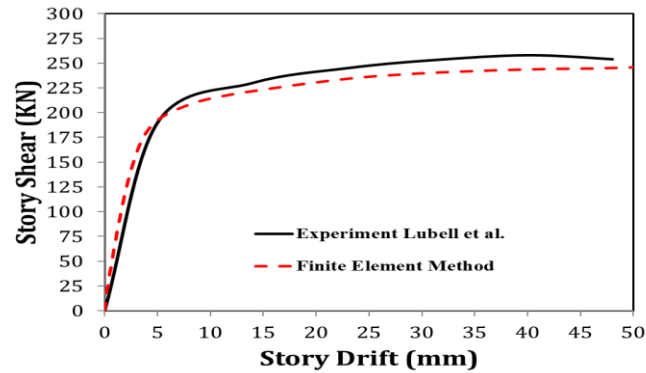


Fig. 4. Comparison of finite element method with experimental results.

3. Results of nonlinear pushover analyses

In the present study, the pushover analysis was conducted on SPSW with various spans of 3m, 4.5m 6m, and 7.5m. Each finite element model had three types of steel plates: low-yield (S100), medium-yield (A36) and high-strength (A572) plates. In order to investigate the behaviour of the moment frame, the moment frame of the shear walls was separately analyzed.

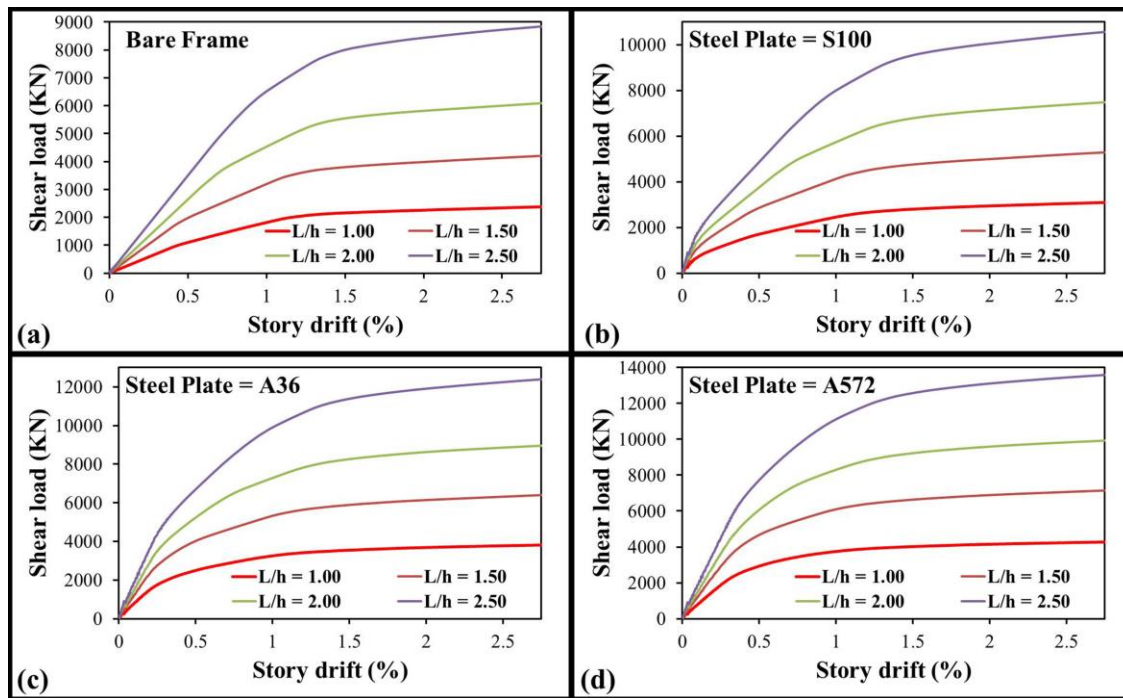


Fig. 5. Pushover analyses results: (a) bare moment frame (b) SPSW with low-yield steel plate (c) SPSW with medium-yield steel plate (d) SPSW with high-strength steel plate.

Fig. 5 illustrates the results of nonlinear pushover of finite element model of SPSW with different steel plates. Moreover, the results of steel moments are shown in the figure as well. It can be seen increasing span length improves shear capacity of the system. Also increasing yield strength of steel plate develops the shear capacity of the system. Fig. 6 shows the Von Mises stress distribution of SPSW with span of 7.5m at drift of 0.33% and 1%.

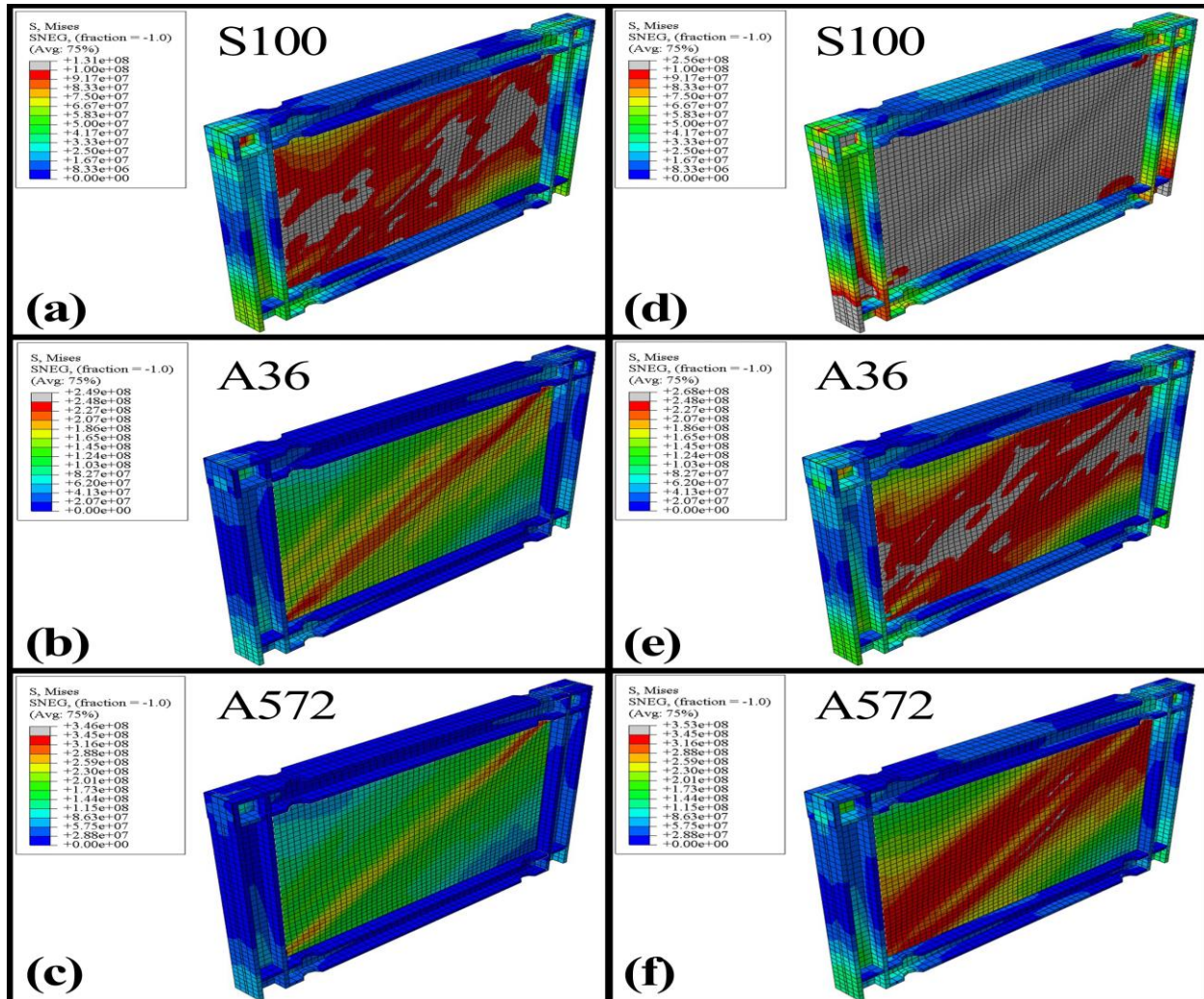


Fig. 6. Von Mises stress distribution: (a) SPSW with low-yield infill steel plate at drift of 0.33% (b) SPSW with low-yield infill steel plate at drift of 1% (c) SPSW with medium-yield infill steel plate at drift of 0.33% (d) SPSW with medium-yield infill steel plate at drift of 1% (e) SPSW with high-strength infill steel plate at drift of 0.33% (f) SPSW high-strength infill steel plate at drift of 1%.

In accordance with Fig 6, the total yield of infill steel plate takes place at drift of 33%, when the low-yield steel plate is used. However, there is partial yield in the steel plate, while the medium- or high-strength steel is utilized. It is noted that the steel plate yields totally at the drift of 1%, when the medium- or high-strength steel is manipulated.

3.1. Investigation of the wall-frame interaction

For the purpose of studying the wall-frame interaction, the base shear of SPSW and the moment frame with RBS beams are initially calculated through Pushover analysis. Subsequently, the shear force in the infill plate is found by calculating the difference of the base shear between the wall and the frame. The plate shear force calculated with the method is similar to integration of software output too. This technique was used by Habashi et al. (2010) and Shafaei et al. (2018) [16–25].

Fig. 7-9 show shear capacity of steel shear wall, steel plate, and moment frame with RBS beams. Additionally, the wall-frame interactions are also illustrated in the figures. It can be seen in the diagrams of the base shear of the finite element models that by increase of the infill steel plate strength, the shear capacity will also increase. The diagrams of the contribution of the steel plates and the frames to the drift will verify this finding that using high-strength steel plate in shear wall will enhance the contribution of the infill plate, as shown in Fig. 9.

The wall-frame interaction diagrams of the shear wall and the moment frames indicate that at the initial loading stage, the steel plate receives 70-80 percent of the lateral forces. However, by increase of the lateral force, the contribution of the steel plate lowers accordingly. When the steel plate yields and the lateral force of the structure exceeds its internal strength capacity, then the shear capacity of the moment frame absorbs more lateral force. During the time that the shear force is being tolerated by the moment frame, increase of the drift causes plastic hinges in the column base or on the RBS beams. By further increase of the force and occurrence of large drifts, the structure fails, and its bending capacity reduces significantly and approaches toward zero. The behaviour is similar to the reported behaviour by Habashi et al. (2010) and Shafaei et al. (2018) [16–25].

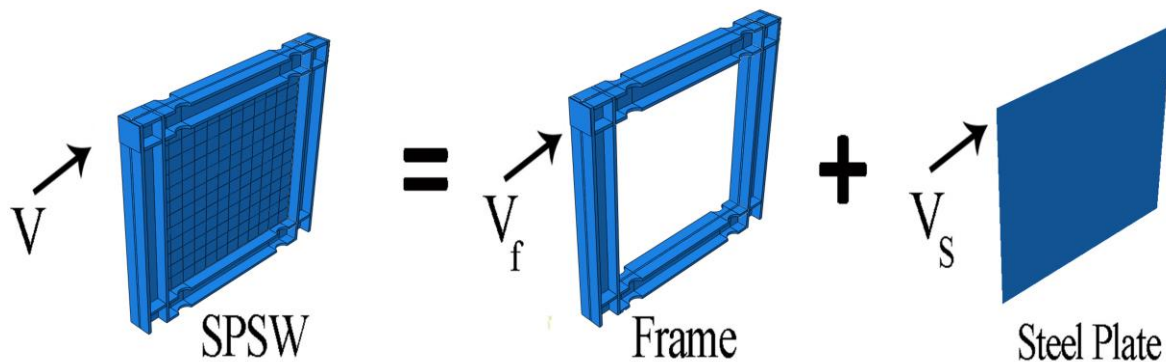


Fig. 7. Components of SPSW (Wall-Frame interaction).

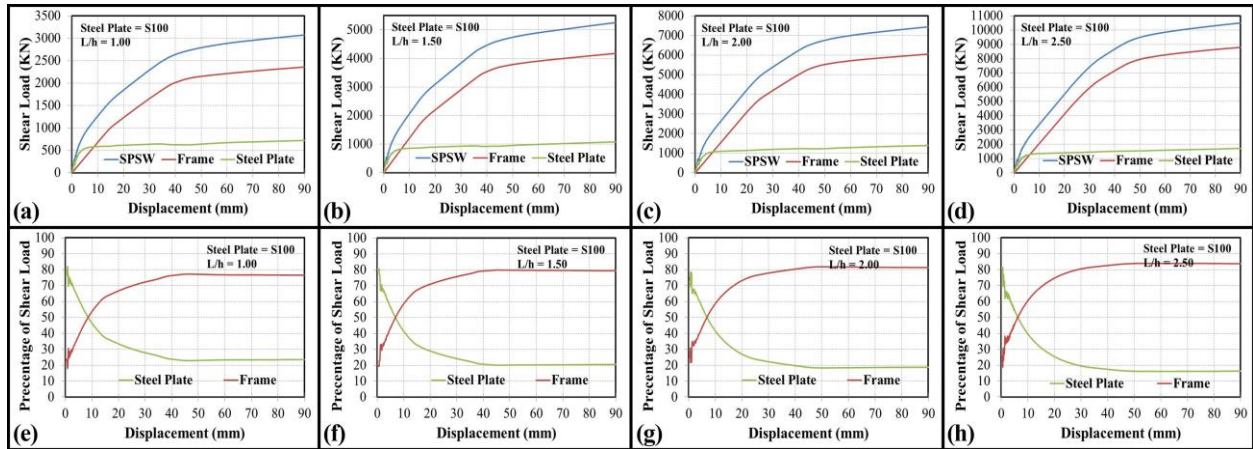


Fig. 7. “Shear load-story drift” and “wall-frame interaction” curves of all SPSWs and moment frame using low-yield infill plate with different spans (3m, 4.5m, 6m, and 7.5m).

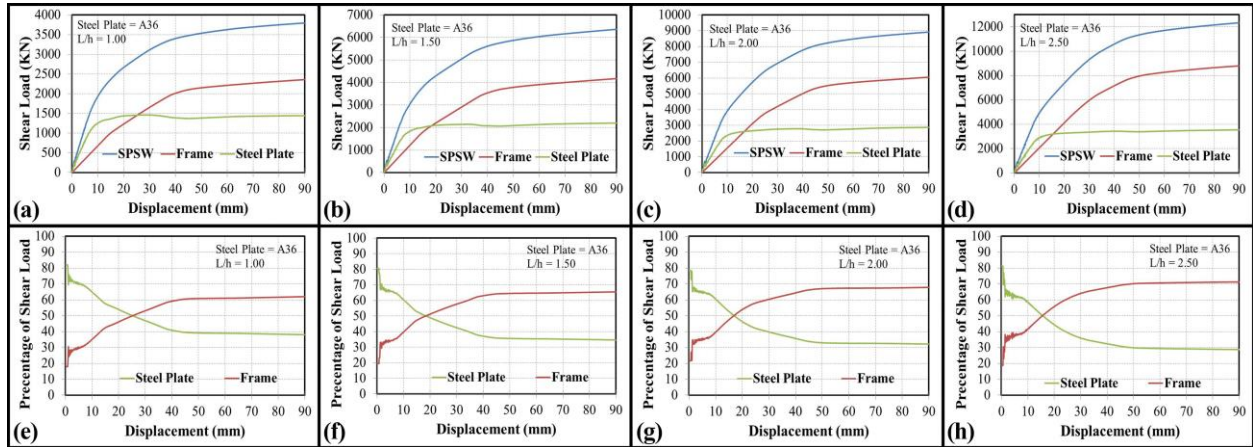


Fig. 8. “Shear load-story drift” and “wall-frame interaction” curves of all SPSWs and moment frame using medium-yield infill plate with different spans (3m, 4.5m, 6m, and 7.5m).

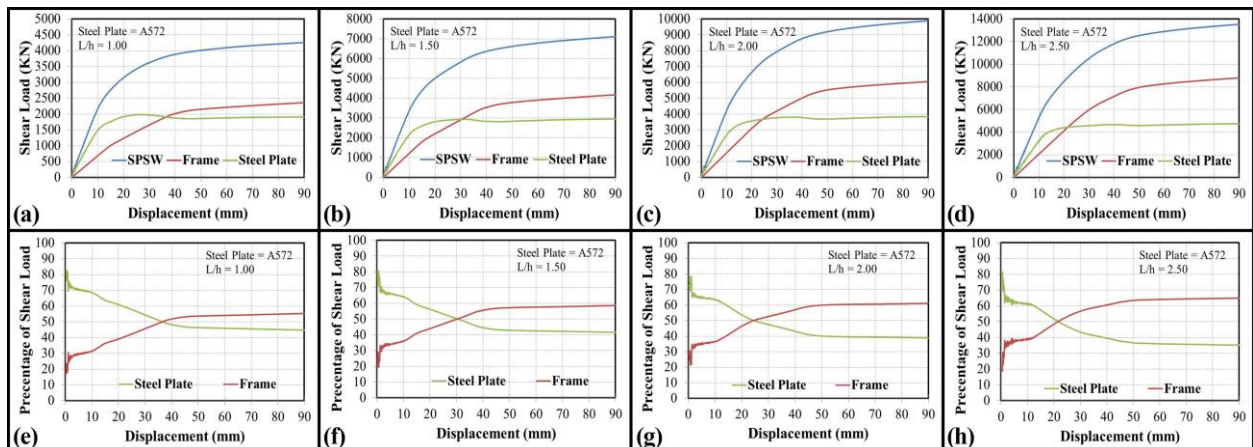


Fig. 9. “Shear load-story drift” and “wall-frame interaction” curves of all SPSWs and moment frame using high-strength infill plate with different spans (3m, 4.5m, 6m, and 7.5m).

4. Seismic structural properties

4.1. Ultimate shear capacity

The ultimate shear capacity is an important parameter in the design of the shear walls. Based on ASCE7 the ultimate shear capacity is equal to the walls' strength at the 2.5% drift. Fig. 10 shows the ultimate shear capacity of the finite element models. Additionally, Table 2 presents the following parameters: the ultimate shear capacity, the difference of the wall strength to the frame, and the percentage of the increased strength. It can be seen in this table that, unlike the high-strength steel, using low-yield steel plate lowers the ultimate shear capacity of the wall. In addition, Table 2 indicates that by increasing the span, the shear capacity will increase, but the percentage of the strength capacity reduces in compare to the frame. For example, in the case of low-yield plate, by increasing the span from 3m to 7.5m, the ultimate capacity enhances from 2988.32 KN to 10202.10 KN, but the percentage of the strength difference between the wall and the frame will reduce from 23.38% to 16.14%.

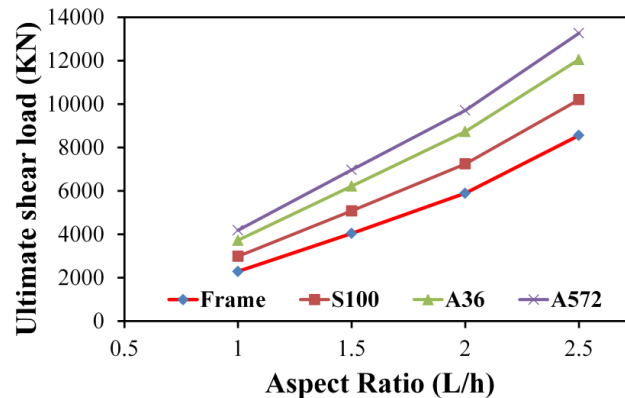


Fig. 10. The ultimate shear capacity of the finite element models.

Table 2

The ultimate shear capacity of the finite element models.

F.E. Model	Ultimate strength (KN)	Diff. of the ult. Str. of wall to frame	Difference(%)
S3-S100-A1.0	2988.32	698.55	23.38
S3-S100-A1.5	5077.39	1035.02	20.38
S3-S100-A2.0	7242.12	1347.48	18.61
S3-S100-A2.5	10202.10	1646.36	16.14
S3-A36-A1.0	3725.55	1435.78	38.54
S3-A36-A1.5	6217.83	2175.46	34.99
S3-A36-A2.0	8735.45	2840.81	32.52
S3-A36-A2.5	12053.20	3497.46	29.02
S3-A572-A1.0	4189.83	1900.06	45.35
S3-A572-A1.5	6970.25	2927.88	42.01
S3-A572-A2.0	9707.95	3813.31	39.28
S3-A572-A2.5	13264.90	4709.16	35.50

4.2. Lateral stiffness

Fig. 11 shows the lateral stiffness of steel shear walls and moment frames. According to the figure, in a specific span, the initial elastic stiffnesses of steel plate shear walls are the same regardless of strength of infill steel plate. Moreover, when the drift ratio goes beyond of 1%, the lateral stiffness of shear walls and frames are similar. The reason is that infill steel plate is not active after that drift ratio.

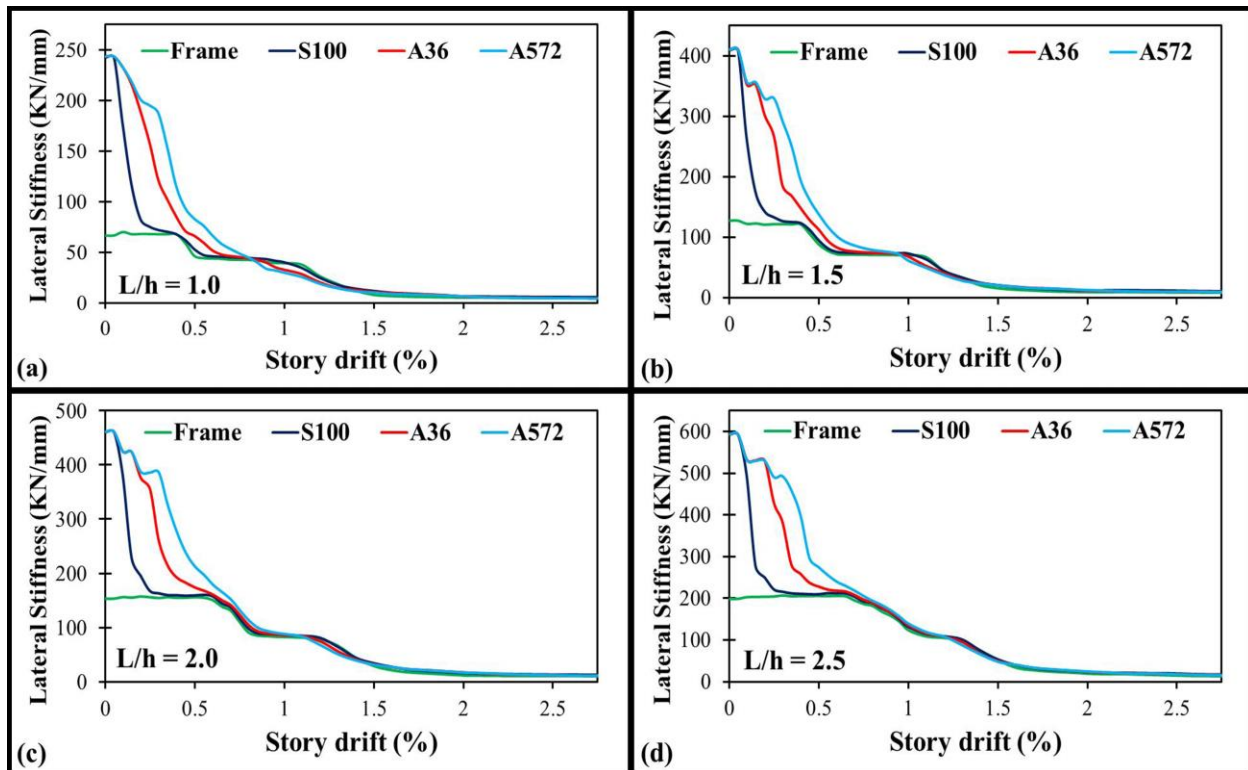


Fig. 11. lateral stiffness of finite element models of SPSW and moment frame with different spans (3m, 4.5m, 6m, and 7.5m).

4.3. Ductility

The ductility of the shear wall is measured based on the constant energy theory. It is assumed that the shear wall has a bilinear elastic-plastic behaviour, so the yield displacement was calculated. Fig. 12 represents the idealized diagram of the behaviour of steel shear wall. Ductility of the finite element models are calculated using this idealized behaviour diagram, and results are shown in Fig. 13. As it can be seen in the figure, the shear walls with low-yield steel plate have high ductility capacity, and this is an advantage of using such steel plates.

Likewise, Table 3 gives the ductility of the finite element models. It can be seen in this table that by increase of the wall span, the ductility of SPSW decreases. Also, in the case that low-yield steel plate is used, the difference of the ductility of wall and frame is almost 3.5 to 4.5, which is a significant difference. In addition, the ductility ratio of the SPSW is almost 65% higher than the moment frames using RBS beams.

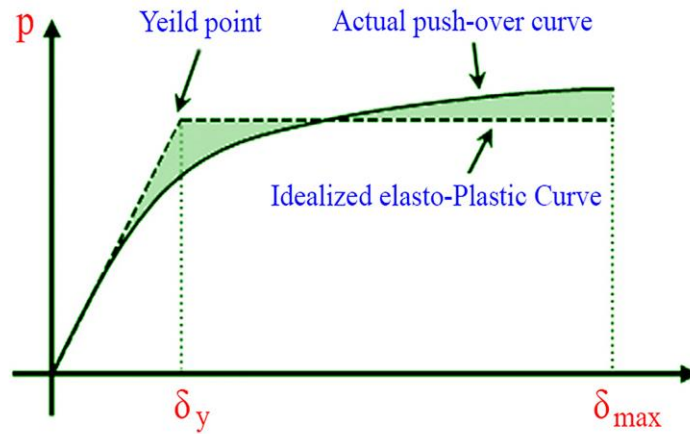


Fig. 12. The idealized diagram of the behavior of the steel shear wall.

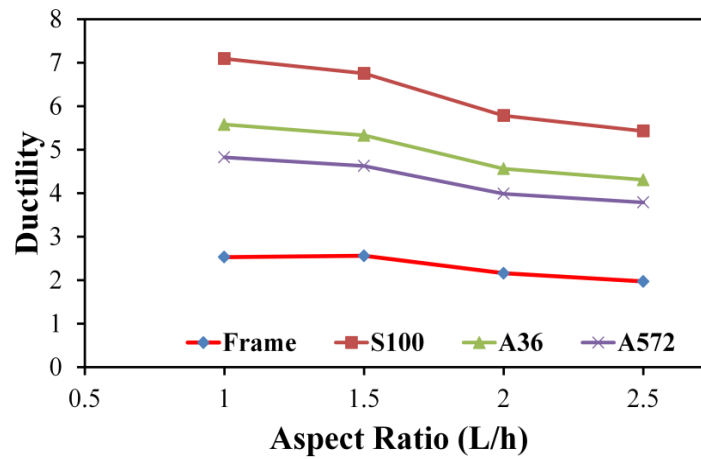


Fig. 13. Ductility of the finite element models of SPSW and moment frame with different spans (3m, 4.5m, 6m, and 7.5m).

Table 3

Ductility of the finite element models.

F.E. Model	Ductility		
S3-S100-A1.0	7.09	4.56	64.32
S3-S100-A1.5	6.75	4.19	62.08
S3-S100 -A2.0	5.78	3.62	62.63
S3-S100-A2.5	5.43	3.46	63.67
S3-A36-A1.0	5.58	3.05	54.65
S3-A36-A1.5	5.33	2.77	51.95
S3-A36-A2.0	4.56	2.40	52.64
S3-A36-A2.5	4.31	2.34	54.22
S3-A572-A1.0	4.82	2.29	47.55
S3-A572-A1.5	4.63	2.07	44.66
S3-A572-A2.0	3.99	1.83	45.80
S3-A572-A2.5	3.79	1.82	47.96

4.4. Energy absorption

The energy absorption of the finite element models is calculated in this study, as shown in Fig. 14. The amount of absorbed or dissipated energy in SPSW is measured based on the integral of the area of the shear-displacement diagram. Table 4 presents the energy absorption of the finite element models, their ductility difference with moment frames with RBS beams, and the percentage of difference. It can be seen in the table that using high-strength infill steel plate will increase the energy absorption. Likewise, increasing the wall span improve both energy absorption and dissipation.

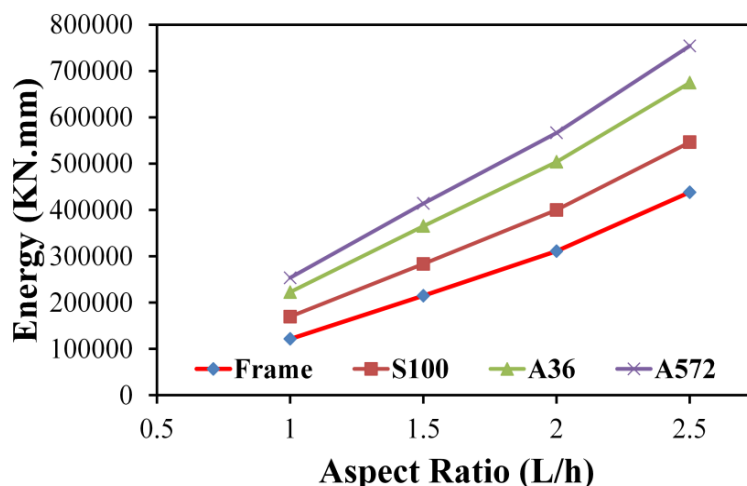


Fig. 14. The energy absorbed by the finite element models.

Table 4

Energy absorption of the finite element models.

F.E. Model	Ductility	Ductility difference with frame	Difference (%)
S3-S100-A1.0	169635.06	48134.64	28.38
S3-S100-A1.5	283259.67	68563.13	24.21
S3-S100 -A2.0	399820.51	88786.35	22.21
S3-S100-A2.5	546023.66	107964.87	19.77
S3-A36-A1.0	222467.10	100966.68	45.38
S3-A36-A1.5	365088.72	150392.18	41.19
S3-A36-A2.0	503804.31	192770.16	38.26
S3-A36-A2.5	674599.20	236540.41	35.06
S3-A572-A1.0	253360.93	131860.51	52.04
S3-A572-A1.5	413918.15	199221.61	48.13
S3-A572-A2.0	566420.28	255386.12	45.09
S3-A572-A2.5	754083.12	316024.33	41.91

5. Conclusion

In the present study, the wall-frame interaction of the steel shear walls with the moment frames using RBS beams is scrutinized by finite element method. For this purpose, the low-yield,

medium-yield and high-strength steel plates were used in the shear wall of finite element models. The SPSW behaviour was compared to its bare moment frame.

The Pushover analysis was conducted on the finite element models and the seismic important parameters, including the lateral stiffness, the ultimate shear capacity, energy absorption and ductility are investigated.

Results of the study indicate the effect of using low-yield steel plate is indirectly proportional to the wall-frame interaction of the wall and the moment frame and reduces the shear capacity of the infill plate of the web, whereas the effect of using high-strength steel enhances the shear capacity of the infill plate of the web. Moreover, using different steels will not change the initial elastic lateral stiffness. However, the lateral stiffness of the shear wall is higher than the moment frame with RBS beams. Moreover, after the drift of 1%, the stiffness of the system is provided by moment frame.

Furthermore, it was observed that by increase of the shear wall span, the ultimate strength and energy dissipation of the shear wall will significantly increase, but the ductility will decrease. In ductility analysis, it was also revealed that the shear wall has 65% higher ductility capacity than the moment frame with RBS beams. In addition, the results unveiled that using low-yield steel plate improves the ductility capacity, whereas high-strength steel plates improve the energy absorption capacity of the shear wall.

References

- [1] Sabelli R, Bruneau M. Steel Plate Shear Walls, American Institute of steel construction. Inc AISC Steel Des Guid 2006;20:1–21.
- [2] Vian D, Bruneau M, Tsai K-C, Lin Y-C. Special perforated steel plate shear walls with reduced beam section anchor beams. I: Experimental investigation. *J Struct Eng* 2009;135:211–20.
- [3] Astaneh-Asl A. Seismic behavior and design of steel shear walls 2001.
- [4] Association CS. Limit states design of steel structures—CAN/CSA-S16. 1-94. Rexdale, Ontario Can Stand Assoc 1994.
- [5] Construction AI of S. Seismic provisions for structural steel buildings. American Institute of Steel Construction; 2002.
- [6] Driver RG, Kulak GL, Kennedy DJL, Elwi AE. Cyclic test of four-story steel plate shear wall. *J Struct Eng* 1998;124:112–20.
- [7] Jahanpour A, Moharrami H, Aghakoochak A. Evaluation of ultimate capacity of semi-supported steel shear walls. *J Constr Steel Res* 2011;67:1022–30. doi:10.1016/j.jcsr.2011.01.007.
- [8] Jahanpour A, Jönsson J, Moharrami H. Seismic behavior of semi-supported steel shear walls. *J Constr Steel Res* 2012;74:118–33. doi:10.1016/j.jcsr.2012.02.014.
- [9] Alinia MM, Hosseinzadeh SAA, Habashi HR. Buckling and post-buckling strength of shear panels degraded by near border cracks. *J Constr Steel Res* 2008;64:1483–94. doi:10.1016/j.jcsr.2008.01.007.
- [10] Amiri B, AghaRezaei H, Esmaeilabadi R. The Effect of Diagonal Stiffeners on the Behaviour of Stiffened Steel Plate Shear Wall. *J Comput Eng Phys Model* 2018;1:58–67.
- [11] Zhao Q, Astaneh-Asl A. Cyclic Behavior of Traditional and Innovative Composite Shear Walls. *J Struct Eng* 2004;130:271–84. doi:10.1061/(ASCE)0733-9445(2004)130:2(271).

- [12] Shafaei S, Ayazi A, Farahbod F. The effect of concrete panel thickness upon composite steel plate shear walls. *J Constr Steel Res* 2016;117:81–90. doi:10.1016/j.jcsr.2015.10.006.
- [13] Rassouli B, Shafaei S, Ayazi A, Farahbod F. Experimental and numerical study on steel-concrete composite shear wall using light-weight concrete. *J Constr Steel Res* 2016;126:117–28. doi:10.1016/j.jcsr.2016.07.016.
- [14] Ayazi A, Ahmadi H, Shafaei S. The effects of bolt spacing on composite shear wall behavior. *World Acad Sci Eng Technol* 2012;6:10–27.
- [15] Shafaei S, Farahbod F, Ayazi A. Concrete Stiffened Steel Plate Shear Walls With an Unstiffened Opening. *Structures* 2017;12:40–53. doi:10.1016/j.istruc.2017.07.004.
- [16] Shafaei S, Farahbod F, Ayazi A. The wall-frame and the steel-concrete interactions in composite shear walls. *Struct Des Tall Spec Build* 2018;27:e1476. doi:10.1002/tal.1476.
- [17] Arabzadeh A, Soltani M, Ayazi A. Experimental investigation of composite shear walls under shear loadings. *Thin-Walled Struct* 2011;49:842–54. doi:10.1016/j.tws.2011.02.009.
- [18] Guo L, Li R, Rong Q, Zhang S. Cyclic behavior of SPSW and CSPSW in composite frame. *Thin-Walled Struct* 2012;51:39–52. doi:10.1016/j.tws.2011.10.014.
- [19] Shafaei S, Rassouli B, Ayazi A, Farahbod F. Nonlinear behavior of concrete stiffened steel plate shear wall. *7th Int. Conf. Seismol. Earthq. Eng. Tehran, Iran, 2015*, p. 18–21.
- [20] Ayazi A, Farahbod F, Rassouli B, Shafaei S. Experimental research on concrete stiffened steel plate shear wall. *7th Int. Conf. Seismol. Earthq. Eng. Tehran, Iran, 2015*, p. 18–21.
- [21] Sabouri-Ghomi S, Ventura CE, Kharrazi MH. Shear Analysis and Design of Ductile Steel Plate Walls. *J Struct Eng* 2005;131:878–89. doi:10.1061/(ASCE)0733-9445(2005)131:6(878).
- [22] Berman JW, Bruneau M. Experimental investigation of light-gauge steel plate shear walls for the seismic retrofit of buildings 2003.
- [23] Hosseinzadeh SAA, Tehranizadeh M. Introduction of stiffened large rectangular openings in steel plate shear walls. *J Constr Steel Res* 2012;77:180–92. doi:10.1016/j.jcsr.2012.05.010.
- [24] Lubell AS, Prion HGL, Ventura CE, Rezai M. Unstiffened Steel Plate Shear Wall Performance under Cyclic Loading. *J Struct Eng* 2000;126:453–60. doi:10.1061/(ASCE)0733-9445(2000)126:4(453).
- [25] Habashi HR, Alinia MM. Characteristics of the wall–frame interaction in steel plate shear walls. *J Constr Steel Res* 2010;66:150–8. doi:10.1016/j.jcsr.2009.09.004.
- [26] ABAQUS Analysis user's manual, version 6.10. n.d.